Chronobiology International, 2014; 31(5): 668–679
© Informa Healthcare USA, Inc.
ISSN: 0742-0528 print / 1525-6073 online
DOI: 10.3109/07420528.2014.886588

informa
healthcare

ORIGINAL ARTICLE

Modulation of mammalian circadian rhythms by tumor necrosis factor-α

Natalia Paladino, Malena L. Mul Fedele, José M. Duhart, Luciano Marpegan, and Diego A. Golombek

Laboratorio de Cronobiología, Universidad Nacional de Quilmes, Buenos Aires, Argentina

Systemic low doses of the endotoxin lipopolysaccharide (LPS, 100 μg/kg) administered during the early night induce phase-delays of locomotor activity rhythms in mice. Our aim was to evaluate the role of tumor necrosis factor (Tnf)-alpha and its receptor 1/p55 (Tnfr1) in the modulation of LPS-induced circadian effects on the suprachiasmatic nucleus (SCN). We observed that Tnfr1-defective mice (Tnfr1 KO), although exhibiting similar circadian behavior and light response to that of control mice, did not show LPS-induced phase-delays of locomotor activity rhythms, nor LPS-induced cFos and Per2 expression in the SCN and Per1 expression in the paraventricular hypothalamic nucleus (PVN) as compared to wild-type (WT) mice. We also analyzed *Tnfr1* expression in the SCN of WT mice, peaking during the early night, when LPS has a circadian effect. Peripheral inoculation of LPS induced an increase in cytokine/chemokine levels (Tnf, Il-6 and Ccl2) in the SCN and in the PVN. In conclusion, in this study, we show that LPS-induced circadian responses are mediated by Tnf. Our results also suggest that this cytokine stimulates the SCN after LPS peripheral inoculation; and the time-related effect of LPS (i.e. phase shifts elicited only at early night) might depend on the increased levels of *Tnfr1* expression. We also confirmed that LPS modulates clock gene expression in the SCN and PVN in WT but not in Tnfr1 KO mice.
Highlights: We demonstrate a fundamental role for Tnf and its receptor in circadian modulation by immune stimuli at the level of the SCN biological clock.

Keywords: Circadian rhythms, lipopolysaccharide, suprachiasmatic nucleus, TNF receptor 1, tumor necrosis factor-alpha

INTRODUCTION

Daily environmental changes have imposed a selective pressure for life on earth, driving the development of a circadian clock mechanism for the generation and entrainment of rhythms in physiological and behavioral variables (e.g. body temperature, hormonal secretion, sleep, locomotor activity, etc.). In mammals, the master clock resides in the hypothalamic suprachiasmatic nucleus (SCN), and the principal signal that adjusts its activity is the light–dark (LD) cycle (Golombek & Rosenstein, 2010).

Although there is substantial information regarding the circadian modulation of many immunological variables (reviewed in Coogan & Wyse, 2008; Leone et al., 2007; Scheiermann et al., 2013), little is known about the possible effect of immune factors on the circadian system itself. In addition, key immune mechanisms might be intrinsically rhythmic, as recently suggested for spleen, lymph nodes and peritoneal macrophages (Bollinger et al., 2011; Keller et al., 2009).

On the other hand, it is well known that the introduction of Gram-negative bacteria into the body causes the liberation of toxic, soluble products of the bacterial cell wall, such as lipopolysaccharide (LPS). Peripheral administration of LPS exerts profound effects on the sleep–wake cycle (one of the most evident circadian rhythms) and may produce fever and a characteristic sickness behavior observed during inflammatory diseases, including changes in sleep patterns (Kluger, 1991; Krueger et al., 1998). In addition, it is now well established that LPS induces autonomic, endocrine and behavioral responses that are controlled by the brain (Linthorst & Reul, 1998; Matsunaga et al., 2000).

In order to investigate the modulatory mechanisms operated by the immune components on the circadian clock, we focused our experiments on the effect of low-dose LPS inoculation as a model of mild immune activation. Systemic low doses of LPS administered at circadian time (CT) 15 (where CT12 corresponds to activity onset in constant darkness) produce a

Submitted November 19, 2013, Returned for revision January 8, 2014, Accepted January 20, 2014

Correspondence: Dr. Diego A. Golombek, Departamento de Ciencia y Tecnología, Universidad Nacional de Quilmes, R. S. Peña 180, 1876 Bernal, Buenos Aires, Argentina. Tel: 54-11-4365-7100 (ext. 5626). Fax: 54-11-4365-7132. E-mail: dgolombek@unq.edu.ar

photic-like phase delay of the locomotor activity rhythm in mice, but it has no significant effect when injected at other CTs (Marpegan et al., 2005). Intracerebroventricular (icv) injections of interleukin (Il)-1b or tumor necrosis factor-α (Tnf-α), which are strongly stimulated by LPS, also induce phase-delays at CT15. Moreover, the Tnf-soluble receptor, but not the Il-1 receptor antagonist (Il-1rn), inhibits the LPS circadian effect, suggesting that this endotoxin may act on the clock by inducing the release of cytokines, which finally act on the SCN (Leone et al., 2012). The induction of cFos in the SCN and the paraventricular hypothalamic nucleus (PVN) (a relay station of the output circadian pathway originating in the SCN) was previously reported after LPS or cytokine administration (Marpegan et al., 2005; Paladino et al., 2010; Sadki et al., 2007). While the complete pathway involved in the circadian LPS responses is unknown, the immune-related transcription factor Nfκb1 (NF-κB) and the LPS receptor Tlr4 seem to be involved in this circadian effect (Marpegan et al., 2005, 2004; Paladino et al., 2010).

As Tnf seems to be involved in the LPS circadian effect on the locomotor activity rhythm, we have characterized the circadian behavior and LPS-induced circadian response in Tnf receptor-deficient (Tnfr1 KO) mice (Pfeffer et al., 1993), and we evaluated the expression of this cytokine and its receptor in the SCN. Our work, together with previously reported results, strongly suggests an important role of the Tnf/Tnfr1 pathway in the LPS-induced circadian effect, acting on the SCN.

MATERIALS AND METHODS

Animals

Adult (2-month old) C57bl/6J wild-type (WT) and Tnfr1 (p55-*Tnfrsf1a*) KO male mice (*Mus musculus*) were raised in our colony. The Tnfr1 KO mice (originally from The Jackson Laboratory – B6.129-*Tnfrsf1a*^{tm1Mak}/J – raised in a C57bl/6J background) were kindly provided by Dr. Silvia Di Genaro (San Luis National University, Argentina). The neomycin cassette present in KO mice in the position 535 of the coding sequence of Tnfr1 was detected by polymerase chain reaction (PCR) as described by The Jackson Laboratory (data not shown). Mice were housed under a 12:12-h LD photoperiod (with lights on at 8 AM and lights off at 8 PM) with food and water *ad libitum*. Mice were transferred to constant darkness (DD) conditions in single cages 20 days prior to the treatments. All animal experiments were carried out in accordance with international ethical standards for the care and use of laboratory animals (Portaluppi et al., 2010).

Behavioral analysis

Mice were housed in individual cages equipped with running wheels, and their locomotor activity circadian rhythm was recorded with a system designed in our laboratory. Wheel revolutions were monitored by magnetic microswitches activated by the wheel and collected every 5 min. Time is expressed as zeitgeber time (ZT), with ZT12 defined as the time of lights off in LD conditions, or CT, with CT12 defined as the moment of locomotor activity onset in DD conditions. Manipulations in DD were performed under dim red light (< 1 lux).

Mice maintained in DD were exposed to a 10-min white light pulse of 100 lux at CT15 or CT22, or injected with 100 μg/kg of LPS (*Escherichia coli* serotype 0111:B4 Sigma-Aldrich, St. Louis, MO) or saline solution (vehicle, VEH) in a volume of 100–150 μl (depending on the mouse weight) by intraperitoneal (ip) route at CT15 or ZT15. Abrupt 6-h advances in the LD schedule were achieved by advancing the time of lights-on and shortening of the dark phase. Conversely, abrupt 6-h delays in the LD schedule were achieved by delaying the time of lights-on and lengthening the dark phase.

All circadian parameters were calculated using the El Temps (version 1.219, University of Barcelona) or the ClockLab software (version 2.61, Actimetrics, Wilmette, IL). In DD conditions, free-running activity periods (τ) were determined by Chi-square periodograms. For activity pattern analysis, individual waveforms were performed using 15 consecutive days in LD or DD condition. Duration of the subjective night (α) was calculated measuring the time length covered by the portion of the curve on top of the activity mean of each individual waveform (using the corresponding τ). Conversely, ρ (duration of the subjective day) was calculated as the time length covered by the portion of the curve under the activity mean. The percentage of total activity occurring during light or dark in LD and α or ρ in DD conditions was calculated as the percentage of the area under the curve of the waveform analysis occurring within the corresponding interval.

Phase shifts were calculated using the 10 previous days and the 10 days after the stimuli (excluding the two cycles immediately after stimulation), and the activity onset was used as a phase marker. Phase shifts were calculated as the difference between the two projected activity onsets. Resynchronization to the new LD cycle, after the 6-hour shifts, was considered fully accomplished when activity onset took place at the new time of lights off ± 15 minutes and reported as the number of days required to resynchronize for each animal. For delays, the resynchronization time was also analyzed taking into account the offset of the activity pattern.

Tissue cytokine detection

Two hours after LPS or VEH ip inoculation at ZT3 or ZT15, mice were sacrificed by cervical dislocation, brains were removed and SCN and PVN regions were carefully dissected under magnifying glass observation. Proteins were homogenized in 0.01 M phosphate buffer saline (PBS) containing a protease inhibitor cocktail (P8340; Sigma-Aldrich), incubated for 15 min at 4 °C and

centrifuged at 12 000 rpm for 15 min. Supernatants were collected and protein concentration was measured using the Qubit™ kit (Invitrogen, Carlsbad, CA). Concentration of the cytokines Tnf, Il-6, Il-12p70, Interferon-gamma (Ifnγ), Il-10 and the chemokine Ccl2 were determined using the cytometric bead array mouse inflammation kit (Becton Dickinson Company, San Jose, CA) according to the manufacturer's protocol.

RNA extraction and real-time PCR

Tissues corresponding to SCN regions were carefully dissected, as described above, from mice under 12:12 LD conditions at ZT3, ZT7, ZT11, ZT15, ZT19 and ZT23. Total RNA was isolated using 100 µl of TRIzol reagent (Life Technologies, Carlsbad, CA) according to the manufacturer's instructions. Fifteen microliters of RNA solutions were quantified using a NanoDrop1000 equipment (Thermo Scientific, Waltham, MA). cDNA was synthesized from 200 ng of total RNA using oligo(dT) primers and the SuperScript™ First-Strand Synthesis System (Invitrogen) according to the manufacturer's protocol. Gene amplification was performed on a real-time PCR instrument Step One Plus (Applied Biosystems, Carlsbad, CA), using 20 µl of final reaction volume containing the following: 1 µl of cDNA as template, 1 × of the Power SYBR Green PCR Master Mix (Applied Biosystems) and the primers Tnfr1-F (5′-ACC AAG TGC CAC AAA GGA AC-3′) and Tnfr1-R (5′-ATT CTG GGA AGC CGT AAA GG-3′) or Gapdh-R (5′-TGC ACC ACC AAC TGC TTA G-3′) and Gapdh-F (5′-GGA TGC AGG GAT GAT GTT C-3′) (GenBiotech, Ciudad Autónoma de Buenos Aires, Argentina) in a final concentration of 400 nM. The cDNA template was amplified in duplicate, with the following conditions: 95 °C for 10 minutes, followed by 40 cycles of 95 °C for 15 seconds and 60 °C for 1 minute. Then the melting curve was obtained between 60 and 95 °C. Relative gene expression was analyzed using the $2^{-\Delta\Delta Ct}$ method, with values from samples collected at ZT3 used for calibration procedures, while *Gapdh* gene was used as reference.

Immunohistochemistry and immunofluorescence

For Per1 and Per2 detection, mice were deeply anaesthetized with an ip cocktail containing ketamine (150 mg/kg) and xylazine (10 mg/kg) after LPS or VEH treatment and perfused intracardially with 4% paraformaldehyde in PBS. For cFos detection, mice were sacrificed by cervical dislocation. Brains were removed carefully, post-fixed overnight, cryoprotected in 30% sucrose in PBS for 24 h and 20–30 µm thick coronal sections were cut with a freezing cryostat and collected in PBS.

For cFos and Per1, free-floating SCN and PVN-containing sections (10 sections/mouse) were blocked with 5% non-fat milk in PBS containing 0.4% Triton X-100 and incubated with primary antisera raised in rabbit against cFos [Santa Cruz Biotechnology (Dallas, TX), 1:4000 (Joshi & Pratico, 2013)] or Per1 [Affinity BioReagents (Waltham, MA), 1:600 (Chilov et al., 2001)] diluted in the same solution, for 48 h at 4 °C. Sections were then treated using the avidin–biotin method with a Vectastain Elite Universal kit containing a biotin-conjugated secondary antibody, avidin and biotin-conjugated horseradish peroxidase (Vector Laboratories, Burlingame, CA) and Vector-VIP peroxidase substrate (SK-4600).

For Per2 immunofluorescence, brain sections were washed in 0.1 M phosphate buffer (PB) 0.03% Triton X-100 (PBT0.03), next in PB 0.3% Triton X-100 (PBT0.3) and again in PBT0.03. Slices were blocked with 10% non-fat milk in PBT0.03 for 1 h and incubated with primary antisera raised in rabbit against Per2 [Alpha Diagnostics (San Antonio, TX), 1:2000 (Field et al., 2000)] diluted in the same solution, for 72 h at 4 °C. Sections were washed and incubated for 1 h at 37 °C with a FITC-conjugated secondary antibody in PBT0.03 (Vector Laboratories; 1:200). Slices were washed and mounted with DAPI-containing medium (Vectashield®, Vector Laboratories).

Cell counting was performed with the ImageJ 1.29 software (NIH) in hypothalamic sections as previously described (Marpegan et al., 2005). Each SCN region was divided in core and shell subregions (as shown in Figure 4C, depicting a solid line surrounding the whole SCN and a dotted line surrounding the core SCN region). Relative expression was calculated dividing the positive cells number of each sample by the average of VEH-inoculated samples of each experiment.

In situ hybridization

Mice were sacrificed by cervical dislocation and brains were rapidly removed and frozen in 2-methylbutane cooled to –35 °C with dry ice for 5 minutes, and 15 µm thick coronal sections through the SCN were cut on a cryostat, mounted onto slides and stored at –80 °C. At the time of assay, slides were warmed to room temperature and fixed with 4% paraformaldehyde in 0.1 M PB (pH 7.4) for 5 min; rinsed in 2 × sodium chloride/sodium citrate (SSC) for 2 min; acetylated in 0.1 M triethanolamine hydrochloride, 0.15 M NaCl (pH 8.0) and 0.25% acetic anhydride for 10 min; rinsed quickly in 2 × SSC; dehydrated in a series of ethanol solutions and delipidated in chloroform for 5 min. After rinsing in ethanol and drying at room temperature, sections were incubated in prehybridization buffer (50% 4 × SSC, 50% deionized formamide) for 1 hour at 37 °C before incubation with 0.5–1 × of 106 cpm/ml 35S-labeled antisense riboprobe in hybridization buffer (20% deionized formamide, 4% dextran sulfate, 0.4% Denhardt's, 0.02% yeast tRNA, 0.2% sheared salmon sperm DNA and 4% SSC 20 ×) overnight at 55 °C. Slides were cooled at room temperature and coverslips removed by rinsing twice in 1 × SSC for 10 min, followed by treatment with 50% formamide/2 × SSC for 5 min at 52 °C. Slides were rinsed twice in 2 × SSC for 5 min each and then incubated in RNAse buffer (0.5 M NaCl, 1 mM Tris pH 8.0, 1 mM

EDTA pH 8.0, 0.1 mg/ml RNAse A) for 30 min at 37 °C. Slides were washed twice in 2 × SSC for 5 min each and incubated in 50% formamide/50% 2 × SSC for 5 min at 52 °C; dehydrated in an ethanol series in 0.1 × SSC; and washed quickly in distilled water, followed by 70% ethanol and air dried. Slides were exposed to X-ray film (Kodak BIOMAX MR) for 7 days. All solutions up to this point were prepared with RNAse-free distilled water. Optical density (OD) of the autoradiographic hybridization signal was measured using the ImageJ 1.29 sofware (NIH). The average OD for each mouse SCN was derived from at least three sections at the middle region of the nucleus.

Statistical analysis

Data are presented as mean ± SEM. Differences between two groups were analyzed by unpaired Student's *t* test or the non-parametric Mann–Whitney test (for data groups with a non-Gaussian distribution). The difference between more than two groups was analyzed by one- or two-way analysis of variance (ANOVA) or the non-parametric ANOVA Kruskal–Wallis test. Post-hoc pairwise comparisons were performed by means of a Bonferroni test. *p* Values of 0.05 or less were considered to be statistically significant. For each experiment, important statistical data are presented in the text and complete statistical parameters are shown in the figure legends.

RESULTS

Circadian response to LPS in Tnfr1 KO mice

We have previously reported a Tnf-dependent circadian effect of peripheral LPS inoculation in mice (Leone et al., 2012). In this study, we analyzed this phenomenon in Tnfr1 KO mice. LPS administration (100 μg/kg, ip) at CT15 induced a significant phase-delay in WT mice (Figure 1; LPS: –0.32 ± 0.09 h, VEH: –0.06 ± 0.05 h, ANOVA: $p<0.05$). This phase delay was completely absent in Tnfr1 KO mice (LPS: –0.01 ± 0.04 h, VEH: −0.03 ± 0.04 h; $p=0.005$). This result confirms the central role of the Tnf pathway in the LPS circadian effect.

Circadian features in Tnfr KO mice

We also analyzed the circadian features of the Tnfr1 KO mice in comparison with WT mice. We observed a slightly longer free-running period in KO mice in comparison with WT animals (Student's *t* test $p<0.01$; Figure 2A and Table 1). The Tnfr1 KO mice exhibited a circadian period of 23.87 ± 0.04 hours, as compared to WT mice with a period of 23.62 ± 0.07 hours. The activity pattern in LD and DD conditions was analyzed with the individual waveforms, and the similarities between WT and KO strains of mice are shown in the average waveforms in Figure 2(B and C). The length of the subjective night (α), the percentage of α on the corresponding period (%α/τ) and the relation between α and ρ (length of subjective day) under DD conditions were similar in both mice strains. In addition, the activity counts and the percentage of nocturnal activity were similar between KO and WT mice both in LD and DD conditions (data not shown). We also analyzed the light response in Tnfr1 KO in comparison with WT mice. The phase delay induced by light pulses applied at CT15, and phase advances at CT22 were similar in both strains of mice. Furthermore, the number of days required to resynchronize to a new LD schedule after a 6 hours delay or advance in the lights on (experimental jet-lag) was similar between KO and WT mice (Table 1).

Tnf and Tnfr1 presence in the SCN

To further characterize the role of Tnf in the circadian response to immune activation, we analyzed cytokine levels in SCN and PVN brain regions after peripheral LPS

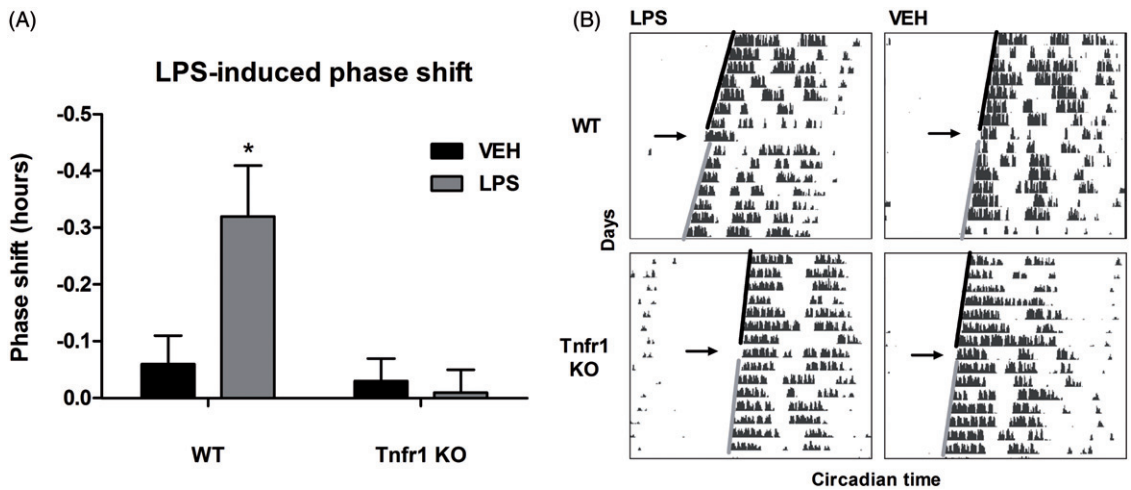

FIGURE 1. LPS-induced phase-delay at CT15 in DD conditions. (A) Mean ± SEM of phase delay after LPS (100 μg/kg, ip) or VEH injection at CT15 in DD condition in WT and Tnfr1 KO mice. (B) Representative actograms. Two-way ANOVA interaction factor: $p<0.05$, strain factor: $p<0.005$, post-hoc comparisons: *$p<0.05$ WT LPS vs all resting groups. WT LPS: $n=11$, WT VEH: $n=11$, KO LPS: $n=7$ and KO VEH: $n=15$. Arrows indicate the inoculation day.

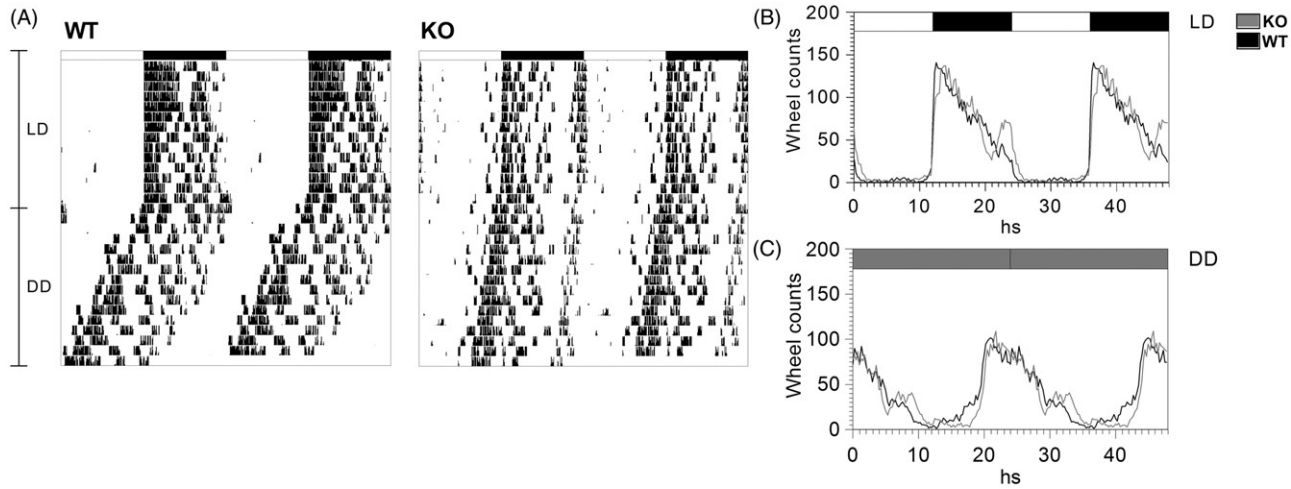

FIGURE 2. Activity patterns of WT and Tnfr1 KO mice. (A) Representative actograms of wheel running activity of WT and Tnfr1 KO mice, in LD and DD conditions. Average waveform of WT and Tnfr1 KO mice in LD (B) and DD (C) conditions. WT: $n=11$ and KO: $n=15$.

TABLE 1. Free-running period and light-response of Tnfr1 KO mice.

	Tnfr1 KO ($n=11$)	WT ($n=10$)	p
τ (hours)[a]	23.87 ± 0.04	23.62 ± 0.07	<0.01
Light-pulse (100 lux)[b]			
CT15 (hours)	–1.6 ± 0.19	–1.9 ± 0.15	ns
CT22 (hours)	0.36 ± 0.08	0.49 ± 0.11	ns
Jet Lag (6 hours)[c]			
Advance (days)	10.3 ± 0.8	8.6 ± 0.7	ns
Delay (days)	4.7 ± 0.2	3.6 ± 0.5	ns

Data are expressed as mean ± SEM. p Values correspond to Student's t test.
[a]Free running period (τ) in DD conditions.
[b]Phase delay at CT15 or phase advance at CT22 induced by a white light pulse (100 lux, 10 minutes).
[c]Time required to resynchronize after a 6-h advance or delay of the LD cycle (jet lag).

inoculation in WT mice. We found increased levels of the cytokines Tnf (ANOVA, $p<0.001$) and Il-6 ($p=0.0001$) and the chemokine Ccl2 ($p<0.001$), 2 hours after LPS ip inoculation in comparison with VEH administration in WT mice, both at ZT3 and at ZT15 in SCN (Figure 3A–C) and PVN (data not shown) regions. The cytokines Il-12p70, Ifnγ and Il-10 were undetectable in both tissues at both times analyzed (data not shown).

As we did not find a time-dependent effect in Tnf levels in the SCN after LPS inoculation, we hypothesized that the restricted time window for the circadian effect of this immune stimulation could depend on the circadian expression of *Tnfr1*. Indeed, *Tnfr1* mRNA levels (assessed by real-time PCR) were higher during the night (Figure 3D), peaking at ZT15 (ANOVA, $p<0.01$). This result suggests that the phase dependency for the LPS-induced circadian effect may be determined by *Tnfr1* circadian expression in the SCN.

Molecular activation of SCN and PVN cells after LPS inoculation

Our next aim was to evaluate the neuronal activation of SCN and PVN brain regions in Tnfr1 KO mice in response to peripheral LPS inoculation. First, we characterized the LPS-induced cFos expression, an early neuronal activation marker, in control animals, at different time intervals (15, 30, 60, 90 minutes and 4 hours) following LPS inoculation. We observed an increase in the number of cFos-positive cells in the core region of the SCN 30 minutes after LPS stimulation (Figure 4A and C; ANOVA; $p<0.01$) and in the shell region 90 minutes after such stimulation (Figure 4B and D; ANOVA; $p<0.005$). Moreover, no difference was observed in cFos expression after an LPS stimulation at ZT3 (data not shown), indicating a time-specific response.

Next, we analyzed the LPS-induced cFos expression in Tnfr1 KO mice. No differences were found in core and shell SCN regions of KO mice after LPS or VEH inoculation, both at 30 and 90 minutes after ZT15 stimulation (Figure 4).

In the PVN region, we found an increased number of cFos-positive cells 90 minutes after LPS inoculation at ZT15 in WT mice (Figure 5; ANOVA $p<0.001$). Moreover, this increase was maintained 4 hours after LPS stimulation (data not shown). When we analyzed cFos expression in the PVN of Tnfr1 KO mice 30 and 90 minutes post inoculation, we did not find any significant difference between LPS and VEH injection.

In addition, expression levels for some components of the circadian clock pathway (Per1, Per2 and Bmal1) were analyzed in brain sections of control and mutant animals (Figures 6 and 7). No difference was found in Per1 expression in the SCN 90 minutes after LPS or VEH inoculation in WT and KO animals (Figure 6). However, we observed a significant increase of Per1 expression in the PVN region of WT mice, but not in KO mice, after LPS inoculation (Figure 6). As expected, light pulses

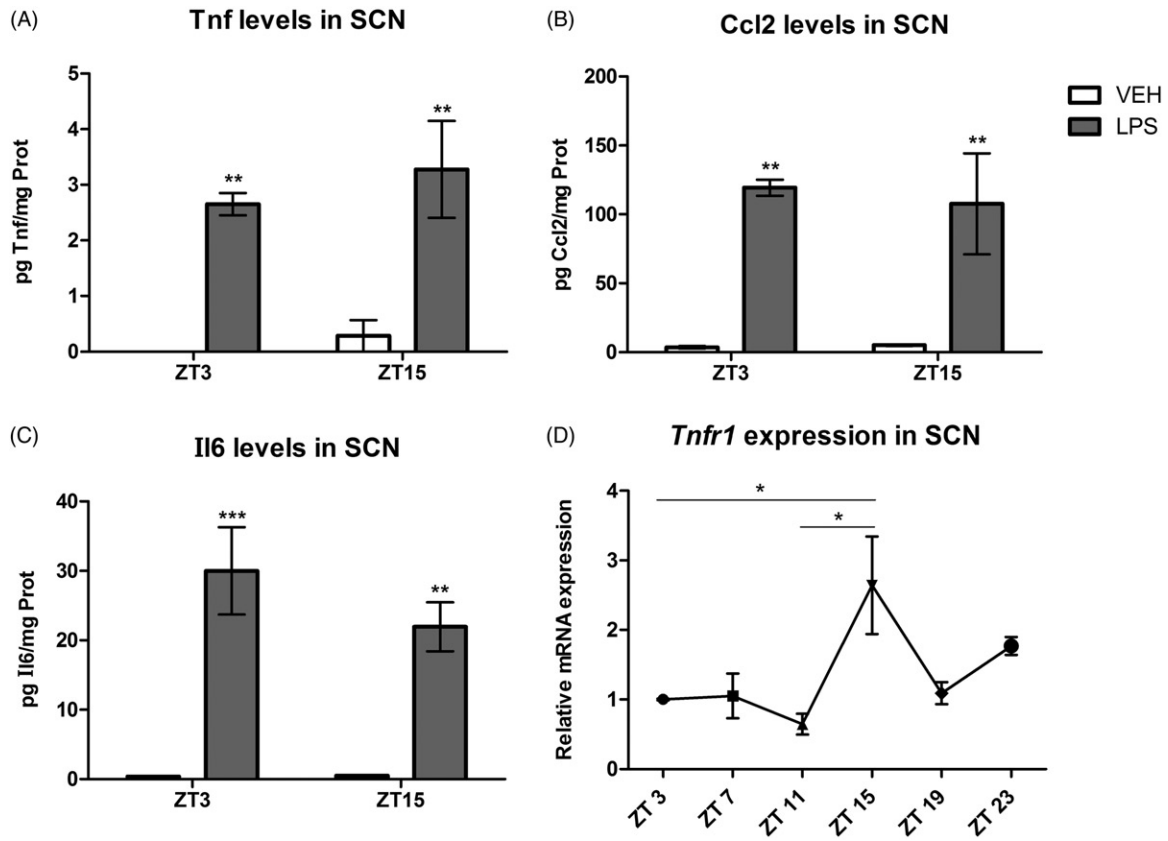

FIGURE 3. LPS-induced cytokines and *Tnfr1* levels in the SCN. Mean ± SEM of pg/mg of protein of Tnf (A), Ccl2 (B) and Il-6 (C) in SCN, 2 hours after LPS (100 μg/kg) or VEH ip inoculation at ZT15 and ZT3 of WT mice, determined by flow cytometry. Two-way ANOVA post-hoc comparisons: $^{**}p<0.01$, $^{***}p<0.001$ LPS vs VEH inoculated mice; $n=3$ (SCN of five mice were pooled for each determination). (D) Mean ± SEM of relative mRNA levels of *Tnfr1* in SCN at different ZTs of WT mice detected by real-time PCR. One-way ANOVA post-hoc comparisons: $^{*}p<0.05$ ZT15 vs ZT3 and ZT11; $n=4$ per time point.

increased *Per1* mRNA expression in the SCN. *Per1* mRNA expression went back to control levels 180 minutes post-light pulses administration at ZT15 (data not shown). In addition, we also performed in situ hybridization to detect *Bmal1* mRNA after LPS or VEH treatment, and we observed a similar OD signal in all groups (data not shown).

We also observed a higher number of Per2-positive cells in core and shell SCN regions in LPS-stimulated WT mice, 150 minutes after inoculation (Figure 7, Student's test: Core $p<0.05$; Shell $p<0.05$). On the contrary, LPS had no effect on Per2 expression in Tnfr1 KO mice.

DISCUSSION

LPS effects on the circadian system

Systemic low doses of LPS delivered at CT15 induce a photic-like phase delay of locomotor activity rhythms in mice (Marpegan et al., 2005). In previous reports, we suggested that LPS may act on the clock by inducing the release of the cytokines Il-1 b and Tnf, which finally act on the SCN (Leone et al., 2006). We recently found that icv delivery of Tnf or Il-1 b induced phase delays on wheel-running activity rhythms. Furthermore, the icv administration of soluble Tnf receptor (but not an Il-1 antagonist) prior to LPS stimulation inhibited phase delays (Leone et al., 2012), confirming the central role of Tnf in the LPS-circadian effect. In order to further characterize this immune-circadian interaction, we analyzed the participation of the Tnf receptor in the LPS-induced phase delay model. In this study, we have studied the circadian behavior and LPS-induced circadian response of Tnfr1 KO mice. We found a Tnfr1-dependent LPS circadian response, both at the behavioral and molecular levels. Interestingly, we observed similar LPS-induced cytokine levels in SCN and PVN brain regions at ZT3 and ZT15, together with an increased level of *Tnfr1* at ZT15 in SCN. These facts suggest a central role of *Tnfr1* circadian expression in the SCN related to the time-dependent LPS effect on biological rhythms.

The phase-shift of locomotor activity rhythms observed after LPS inoculation provides evidence of the response of the circadian system to an immune challenge. Indeed, phase-shifts can be considered as a reliable read-out of the circadian system, because they reflect changes in clock-controlled output variables, and are necessary for the adequate entrainment to the environment. As we used relatively low doses of the

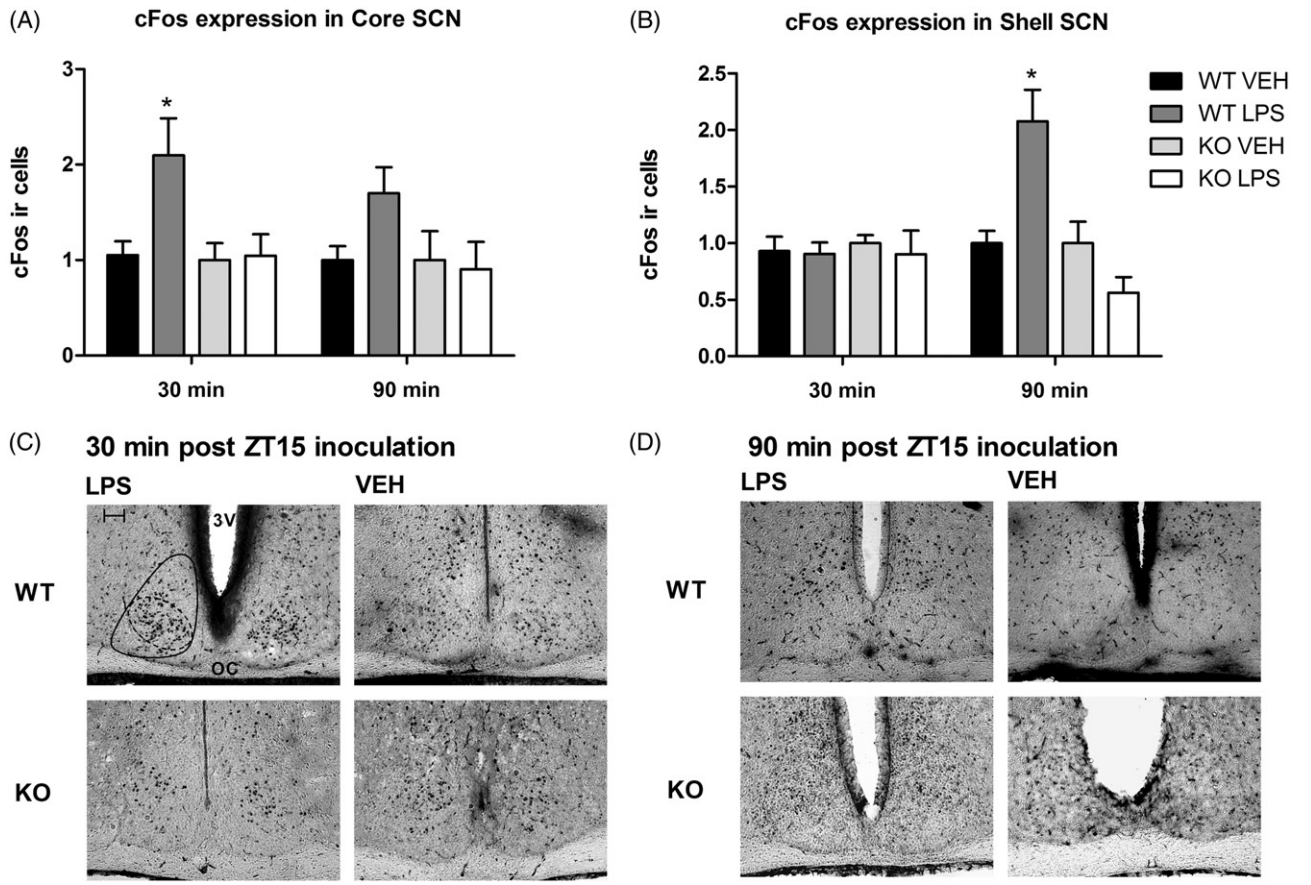

FIGURE 4. LPS-induced cFos expression in the SCN. Immunohistochemistry of cFos in the SCN of mice challenged with LPS (100 μg/kg, ip) or VEH at ZT15. Mean ± SEM of relative number of cFos-positive cells in the core (A) and the shell (B) SCN regions in WT and Tnfr1 KO mice at different time interval post LPS/VEH inoculation. (C and D) Representative pictures of WT and KO mice 30 and 90 minutes after LPS/VEH inoculation. Kruskall–Wallis test: Core 30 minutes; $p<0.01$; Shell 90 minutes: $p<0.005$, post-hoc comparisons: $^*p<0.05$ WT LPS vs all resting groups at the corresponding time. $n=5$–7 per group for 30 minutes and $n=7$–10 per group for 90 minutes. Scale bar = 100 μm. Solid line surrounding the whole SCN and dotted line surrounding the core SCN region. 3 V: third ventricle and OC: optic chiasm.

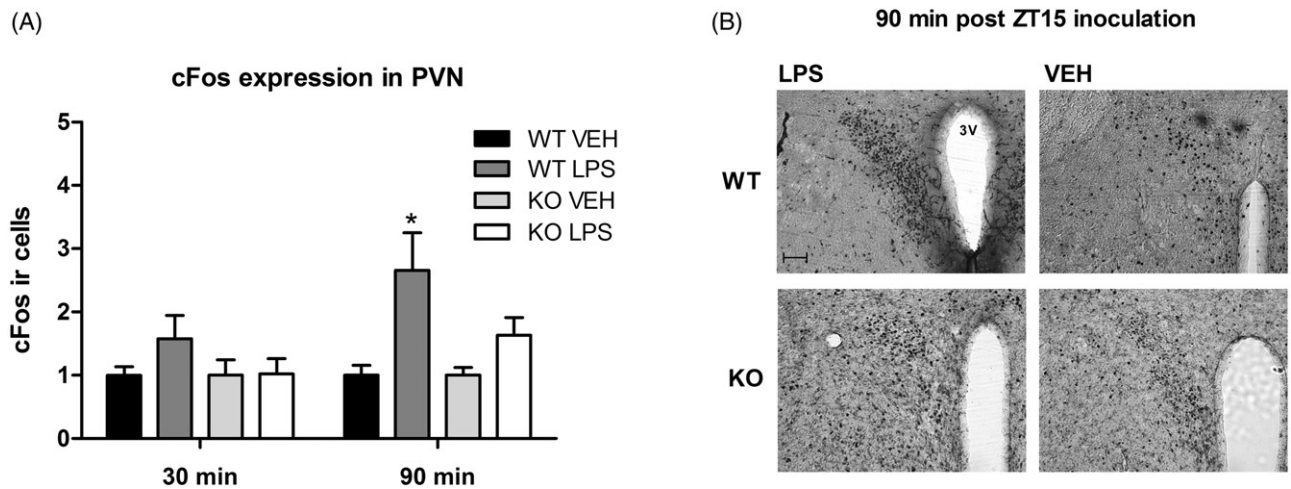

FIGURE 5. LPS-induced cFos expression in the PVN. Mean ± SEM of relative number of cFos-positive cells in the PVN region of WT and Tnfr1 KO mice challenged with LPS (100 μg/kg, ip) or VEH at ZT15 at 30 and 90 minutes post injection (A) and representative pictures (B). (A) 90 minutes: two-way ANOVA post-hoc comparison: $^*p<0.05$ WT LPS vs WT VEH and KO VEH; $n=5$–9 per group. Scale bar = 100 μm. 3 V: third ventricle.

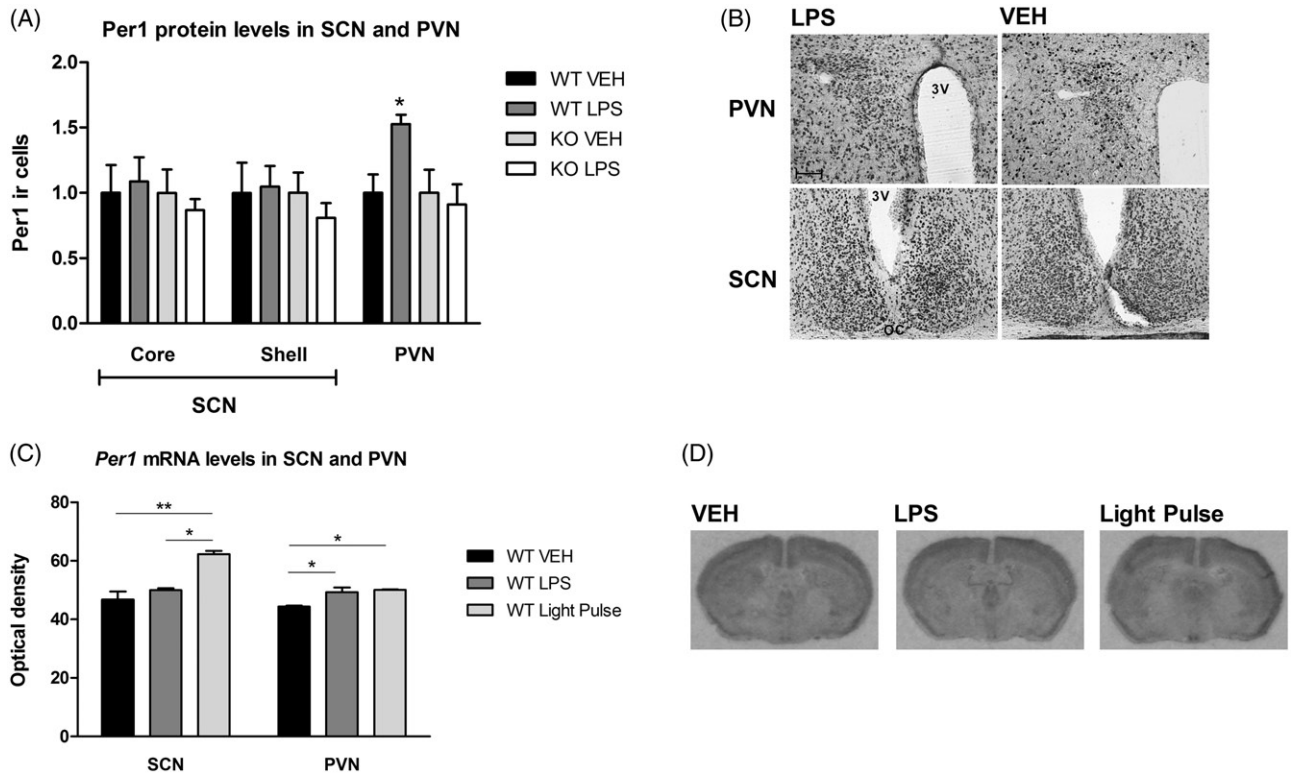

FIGURE 6. LPS-induced Per1 expression in the SCN and the PVN. (A) Mean ± SEM of relative number of Per1-positive cells in the SCN and the PVN region detected by immunohistochemistry, and (B) representative pictures of WT mice challenged with LPS (100 μg/kg, ip) or VEH at ZT15, 90 minutes post inoculation. (C) Mean ± SEM of optical density of *Per1* mRNA signal in the SCN and the PVN regions and (D) representative pictures, detected by *in situ* hybridization in WT mice 90 minutes after LPS/VEH inoculation or 400 lux (10 minutes) of fluorescent white light pulse. (A and B) PVN: Kruskal–Wallis test: $p = 0.01$; post-hoc comparison: $^*p < 0.05$ WT LPS vs WT VEH, KO LPS and KO VEH; $n = 4$–6 animals per group. (C and D) SCN: One-way ANOVA: $p < 0.01$; post-hoc comparison: $^{**}p < 0.01$ WT VEH vs WT light pulse; $^*p < 0.05$ WT LPS vs WT Light Pulse. PVN: one-way ANOVA: $p = 0.02$; post-hoc comparison: $^*p < 0.05$ WT VEH vs WT LPS and WT light pulse; n=3 animals per group. Scale bar = 100 μm. 3 V: third ventricle, OC: optic chiasm.

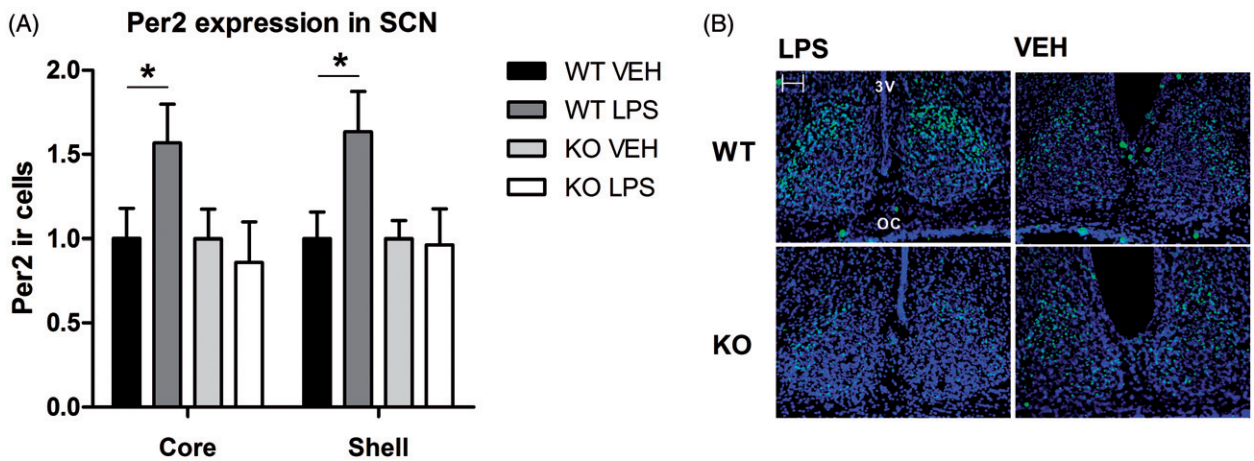

FIGURE 7. LPS-induced Per2 expression in the SCN. (A) Mean ± SEM of relative number of Per2-positive cells in the SCN detected by immunofluorescence and (B) representative pictures, of WT and Tnfr1 KO mice challenged with LPS (100 μg/kg, ip) or VEH at ZT15, 150 minutes post inoculation. Student's t test: WT core: $p < 0.05$; WT shell: $p < 0.05$. WT: $n = 6$, KO: $n = 4$. Scale bar = 100 μm. 3 V: third ventricle and OC: optic chiasm.

endotoxin, this might reflect the modulatory effect of an increased activity of immune effectors on the circadian system. By increasing the release of pro-inflammatory cytokines, LPS might activate a signaling mechanism to the circadian system, and therefore adjust the phase of different clock-controlled variables. In this sense, the endotoxin might be considered a zeitgeber that modulates humoral mechanisms that feedback into the clock. A related mechanism could be activated in response to infections or non-infectious inflammatory diseases, with

the important difference of the chronic stimulation of the immune system. Indeed, increased levels of pro-inflammatory cytokines may affect the circadian system and modify clock-controlled variables. However, the chronic effect of these molecules on the clock could differ from an acute phase modification.

As previously reported, peripheral LPS inoculation induces a phase-response curve similar to the one observed for the light pulses, inducing phase-delays in the early subjective night, in particular at CT15 (Marpegan et al., 2005). We recently reported similar plasma levels of Il-1 a, Il-1 b, Il-6 and Tnf after low doses of LPS inoculation at ZT3 and ZT15 (Leone et al., 2012). Moreover, in this study, we observed similarly increased levels of the cytokines Tnf and Il-6 and the chemokine Ccl2 in the SCN after peripheral LPS inoculation both at ZT3 and at ZT15.

Interestingly, we found a rhythmic expression of *Tnfr1* in SCN, showing an acute peak at ZT15. Our results lead us to propose that the time-dependent effect of LPS or Tnf on the circadian system could be due, at least in part, to the rhythmic expression of this cytokine receptor in the SCN. Similarly, Beynon & Coogan (2010) recently reported a rhythmic expression of Il-1 receptor (Il-1 r) in mice SCN. However, the Il-1 r expression showed increased levels only during the late night.

On the other hand, there are data suggesting that the immune-related transcription factor Nfκb1 is implicated in this response, and its presence and activity in the SCN have been demonstrated for both light and LPS-induced phase shifts (Marpegan et al., 2005, 2004). It is known that Tnf and Il-1 b activate this transcription factor, which induces the expression of Il-6 and Ccl2 (Harada et al., 2011; Kroon et al., 2013; Poon et al., 2013). In addition, Il-6 (which also induces Ccl2 expression) synthesis is regulated through the activation of others transcription factors such as Cebpb (CAAT/enhancer-binding protein beta) and Jun (activator protein 1) (Mogensen, 2013; Waldner et al., 2012). We have reported previously that astrocytes may mediate input signals to mouse SCN coming from the immune system *via* Nfκb1 signaling (Leone et al., 2006). Indeed, we recently observed that SCN astrocytes secrete the cytokines Il-6, Tnf and Ccl2, after Tnf *in vitro* stimulation (Duhart et al., 2013), suggesting that glial cells might represent an interface between the immune and the circadian systems.

Taken together, these data suggest that immune signals might stimulate the SCN independently of the time of day; however, circadian expression of the *Tnfr1* might be responsible for the circadian changes in immune-induced phase shifts in the SCN.

LPS-related pathways within the central nervous system

The mechanism by which peripheral administration of LPS affects the central nervous system (CNS) remains controversial. It has been shown that a dose of 50 μg/kg of LPS can modify core-body temperature and induce sickness behavior in mice (including a decrease in locomotor activity, anhedonia and anorexia), 2–4 hours after stimulation when applied during the early day (Dogan et al., 2000; Lacosta et al., 1999; Teeling et al., 2007). In addition, the change in locomotor activity was observed 2 hours after the ip inoculation of the cytokines Il-1 b, Il-6 and Tnf (Skelly et al., 2013).

LPS (100 μg/kg) is not able to cross the blood–brain barrier (BBB) in rats but it can bind to specific receptors in the cerebral vascular endothelium, inducing proinflammatory responses (Singh & Jiang, 2004). Cerebral expression of Tlr4 has been demonstrated in rat circumventricular organs and in some parenchymal structures, especially within the regions lining the cerebroventricular systems, including the PVN of the hypothalamus (Laflamme & Rivest, 2001). Moreover, cytokines induced peripherally by LPS may also enter the brain through the organum vasculosum laminae terminalis where the BBB is leaky due to the presence of a fenestrated endothelium (Romanovsky et al., 2003) or may act through neural terminals of peripheral tissue, e.g. those of the vagus nerve (Maier et al., 1998; Simons et al., 1998). In this study, we report increased levels of Il-6, Tnf and Ccl2 both in SCN and PVN brain regions after peripheral LPS inoculation. It has been suggested that the chemokine Ccl2 can weaken the BBB and allow other macromolecules to cross into the brain (Yao & Tsirka, 2014). Furthermore, the LPS-induced activation of Il-1 b and Tnf in the brain cortex and hippocampus is dependent on Ccl2 expression, while the inflammatory peripheral response is exaggerated when this chemokine is absent (Thompson et al., 2008).

cFos induction in the PVN after LPS peripheral inoculation has been explored widely (Bienkowski & Rinaman, 2008; Garcia-Bueno et al., 2009; Singru et al., 2008). These nuclei have been described as an output relay station for the SCN (Kalsbeek et al., 2010), and its stimulation affects clock-controlled rhythms such as pineal melatonin secretion (Isobe & Nishino, 2004). We found an increase in cFos expression in this brain region 90 minutes and 4 hours after LPS inoculation at ZT15. The increase of Per1 positive cells number in this brain region at ZT15 (this study) and at ZT22 (Takahashi et al., 2001) suggest that the PVN responds to immune stimulation regardless of time-of-day. In addition, nonphotic circadian phase shifting stimuli have been found to induce Per1 expression in the PVN but not in the SCN (Meza et al., 2008). On the other hand, cFos and Per1 induction in the PVN after LPS stimulation is dependent on the presence of the Tnfr1. The role of LPS-induced clock genes in the PVN for circadian entrainment remains to be examined in more detail.

Circadian responses in Tnfr KO mice

We also analyzed the circadian behavior of Tnfr1 KO mice. Under DD conditions, circadian rhythms assume free-running periods that are close to 24 hours. While

the free-running period in BALB/c mice is close to 23 hours (Shimomura et al., 2001), in C57bl/6 and C57bl/10 mice, it ranges between 23.3 and 23.9 hours (Schwartz & Zimmerman, 1990). In line with this report, we found a free-running period of 23.62 ± 0.07 in the C57bl/6 J control mice. The free-running period of Tnfr1 KO mice resulted slightly, but significantly, longer than in WT mice. Although the ability to resynchronize to a 6-hour shift in the LD cycle (both in delayed or advanced schedules) was similar in mutant and control animals, we observed a tendency of a decreased phase-shift after a light-pulse and a longer resynchronization time to a new LD schedule in KO mice, which could be related to the longer free-running period observed in these mutants.

On the other hand, we also analyzed LPS-induced cFos, Per1 and Per2 expression in the SCN of Tnfr1 KO mice. We found no activation for these markers, suggesting that the Tnfr1 is necessary for LPS-induced molecular changes in the circadian clock.

Immune-circadian interaction: from the clock to the body

A role for cytokines in the regulation of the molecular circadian clock has been suggested in several studies. Cavadini et al. (2007) have shown that treatment with Tnf downregulates the expression of E-box-driven clock genes in cultured fibroblasts. Furthermore, the interaction of Tnf with Tnfr1, but not Tnfrsf1b (Tnfr2), leads to fast downregulation of gene expression of *Dbp* and upregulation of negative regulators of the molecular clock, *Per1* and *Per2*, *Cryptochrome 1*, and *Differentiated embryo chondrocytes 1* (Petrzilka et al., 2009). Regarding Per2, we recently reported that Tnf applied to SCN astrocytes cultures from $Per2^{luc}$ knock-in mice altered both the phase and amplitude of Per2 expression rhythms, in a phase-dependent manner (Duhart et al., 2013).

As for the effects of endotoxin on the brain, it has been reported that peripheral LPS injections (50 μg/kg) at ZT22 caused a rapid induction of *Per1*, but not *Per2*, mRNA levels in the mouse PVN without any change of whole SCN and liver mRNA levels (Takahashi et al., 2001). Higher doses of LPS (1 mg/kg) injected at ZT01 suppressed the *Per2* and *Dbp* mRNA levels in SCN and liver tissue in rats (Okada et al., 2008). Sadki et al. (2007) examined the effect of Tnf/Ifnγ icv microinjection on cFos expression in the SCN and reported an interaction between cytokine treatment and cFos expression in core and shell regions of the SCN. In this study, we evaluated the LPS-induced cFos expression in core and shell SCN brain regions from 15 minutes to 4 hours post injection. In control animals, we observed an increase in the number of cFos-positive cells in the core SCN 30 minutes after LPS and in the shell SCN 90 minutes after stimulation at ZT15. This sequential core-shell activation suggests a photic-like response to LPS inoculation. Moreover, we did not observe any difference in cFos expression in the SCN 90 minutes after ZT3 stimulation, indicating a time-specific response. In addition, we analyzed Per1 and Per2 expression in brain sections after LPS inoculation at ZT15 and we found an increase of Per2-, but not Per1-, positive cells in core and shell SCN regions. For Per1 expression, different time-intervals after LPS inoculation should be analyzed to confirm this result. The difference with previous reports (Okada et al., 2008; Takahashi et al., 2001) in SCN Per2 expression may be related to LPS inoculation time (ZT15 vs. ZT22 or ZT01).

Long-term modulation of Per2, but not of Per1, expression was observed in the SCN of post-septic animals (O'Callaghan et al., 2012). Moreover, Per2-deficent mice were relatively insensitive to such inoculation (Liu et al., 2006). In addition, the inoculation of lethal doses of LPS induces an increased mortality rate at ZT11, in comparison with ZT19 (Halberg et al., 1960; Marpegan et al., 2009). Similarly, Tnf peripheral injection also induced an increased mortality rate at ZT6-10 (Hrushesky et al., 1994). As Per2 levels at ZT11 are higher than at ZT19, these results suggest an important role of this clock protein in LPS-induced septic shock.

The Per2 modulation in different peripheral tissues after immune stimulation remains controversial and seems to depend on the specific tissue and the time of inoculation (Westfall et al., 2013). Moreover, the circadian rhythms of both clock and immune-related molecules depend on the specific immune cell-type (Silver et al., 2012a,b). It is possible that central Per2 modulation participates in the temporal signaling to the periphery. Additional work regarding the peripheral impact of this central clock modulation should be performed. Again, it is important to highlight that the low-dose LPS model is a simplified approach to understand the effect of mild immune stimulation on circadian rhythmicity, but is quite different to a pathological situation where the immune system is chronically stimulated. As for the latter, sickness behavior symptoms, including fatigue, mood alterations, depression, sleep disturbances, loss of appetite and cognitive dysfunction, are prevalent in many systemic inflammatory diseases. The cytokines Tnf, ll-1 b and Il-6 have been postulated as mediators of this communication pathway in the CNS. Many of these symptoms are regulated by the circadian clock; for example, the increase in body temperature and the sleep modulation after Il-1 or Il-6 injection in mice differ depending on the time of administration (Morrow & Opp, 2005; Opp & Toth, 1998; Opp et al., 1991). Chronic inflammation, such as the one observed in animal arthritis models, induce changes in locomotor activity and endocrine rhythms (Laste et al., 2013; Sarlis et al., 1992). In autoimmune diseases, such as rheumatoid arthritis, multiple sclerosis or systemic lupus erythematosus, patients exhibit sleep disturbances and changes in melatonin, cortisol, cytokines and clock gene rhythms (Kouri et al., 2013; Lin et al., 2013). Chronic kidney disease patients often

exhibit a deregulated circadian blood pressure rhythm, such as nocturnal non-dipping profile (Farmer et al., 1997), sleep–wake disruption and a decrease in the amplitude of the melatonin rhythm (Koch et al., 2010). On the other hand, *Trypanosoma brucei brucei*-infected rats showed a significant decline in the amplitude, regularity and ''robustness'' of sleep–wake pattern and body temperature rhythms (Lundkvist et al., 2010; Seke Etet et al., 2012). Indeed, more research is needed to completely understand the immune–circadian interaction during the chronic inflammation in different diseases.

In summary, our results show that Tnf and its receptor Tnfr1 represent the main pathway through which LPS modifies the setting of the circadian clock. This pathway may be an important feedback mechanism by which the immune system signals the circadian system under both physiological and pathological conditions.

DECLARATION OF INTEREST

The authors report no conflicts of interest.

Supported by grants from the National Research Council (CONICET), the National Science Agency (ANPCyT) and the National University of Quilmes (UNQ).

REFERENCES

Beynon AL, Coogan AN. (2010). Diurnal, age, and immune regulation of interleukin-1beta and interleukin-1 type 1 receptor in the mouse suprachiasmatic nucleus. Chronobiol Int. 27: 1546–63.

Bienkowski MS, Rinaman L. (2008). Noradrenergic inputs to the paraventricular hypothalamus contribute to hypothalamic-pituitary-adrenal axis and central Fos activation in rats after acute systemic endotoxin exposure. Neuroscience. 156: 1093–102.

Bollinger T, Leutz A, Leliavski A, et al. (2011). Circadian clocks in mouse and human CD4+ T cells. PLoS One. 6:e29801.

Cavadini G, Petrzilka S, Kohler P, et al. (2007). TNF-alpha suppresses the expression of clock genes by interfering with E-box-mediated transcription. Proc Natl Acad Sci USA. 104: 12843–8.

Coogan AN, Wyse CA. (2008). Neuroimmunology of the circadian clock. Brain Res. 1232:104–12.

Chilov D, Hofer T, Bauer C, et al. (2001). Hypoxia affects expression of circadian genes PER1 and CLOCK in mouse brain. FASEB J. 15:2613–22.

Dogan MD, Ataoglu H, Akarsu ES. (2000). Effects of different serotypes of *Escherichia coli* lipopolysaccharides on body temperature in rats. Life Sci. 67:2319–29.

Duhart JM, Leone MJ, Paladino N, et al. (2013). Suprachiasmatic astrocytes modulate the circadian clock in response to TNF-alpha. J Immunol. 191:4656–64.

Farmer CK, Goldsmith DJ, Cox J, et al. (1997). An investigation of the effect of advancing uraemia, renal replacement therapy and renal transplantation on blood pressure diurnal variability. Nephrol Dial Transplant. 12:2301–7.

Field MD, Maywood ES, O'Brien JA, et al. (2000). Analysis of clock proteins in mouse SCN demonstrates phylogenetic divergence of the circadian clockwork and resetting mechanisms. Neuron. 25:437–47.

Garcia-Bueno B, Serrats J, Sawchenko PE. (2009). Cerebrovascular cyclooxygenase-1 expression, regulation, and role in hypothalamic-pituitary-adrenal axis activation by inflammatory stimuli. J Neurosci. 29:12970–81.

Golombek DA, Rosenstein RE. (2010). Physiology of circadian entrainment. Physiol Rev. 90:1063–102.

Halberg F, Johnson EA, Brown BW, Bittner JJ. (1960). Susceptibility rhythm to *E. coli* endotoxin and bioassay. Proc Soc Exp Biol Med. 103:142–4.

Harada Y, Edamatsu H, Kataoka T. (2011). PLCepsilon cooperates with the NF-kappaB pathway to augment TNFalpha-stimulated CCL2/MCP1 expression in human keratinocyte. Biochem Biophys Res Commun. 414:106–11.

Hrushesky WJ, Langevin T, Kim YJ, Wood PA. (1994). Circadian dynamics of tumor necrosis factor alpha (cachectin) lethality. J Exp Med. 180:1059–65.

Isobe Y, Nishino H. (2004). Signal transmission from the suprachiasmatic nucleus to the pineal gland via the paraventricular nucleus: analysed from arg-vasopressin peptide, rPer2 mRNA and AVP mRNA changes and pineal AA-NAT mRNA after the melatonin injection during light and dark periods. Brain Res. 1013:204–11.

Joshi YB, Pratico D. (2013). The involvement of 5-lipoxygenase activating protein in anxiety-like behavior. J Psychiatr Res. 47: 694–8.

Kalsbeek A, Fliers E, Hofman MA, et al. (2010). Vasopressin and the output of the hypothalamic biological clock. J Neuroendocrinol. 22:362–72.

Keller M, Mazuch J, Abraham U, et al. (2009). A circadian clock in macrophages controls inflammatory immune responses. Proc Natl Acad Sci USA. 106:21407–12.

Kluger MJ. (1991). Fever: Role of pyrogens and cryogens. Physiol Rev. 71:93–127.

Koch BC, van der Putten K, Van Someren EJ, et al. (2010). Impairment of endogenous melatonin rhythm is related to the degree of chronic kidney disease (CREAM study). Nephrol Dial Transplant. 25:513–19.

Kouri VP, Olkkonen J, Kaivosoja E, et al. (2013). Circadian timekeeping is disturbed in rheumatoid arthritis at molecular level. PLoS One. 8:e54049.

Kroon J, Tol S, van Amstel S, et al. (2013). The small GTPase RhoB regulates TNFalpha signaling in endothelial cells. PLoS One. 8: e75031.

Krueger JM, Fang J, Taishi P, et al. (1998). Sleep. A physiologic role for IL-1 beta and TNF-alpha. Ann N Y Acad Sci. 856:148–59.

Lacosta S, Merali Z, Anisman H. (1999). Behavioral and neurochemical consequences of lipopolysaccharide in mice: Anxiogenic-like effects. Brain Res. 818:291–303.

Laflamme N, Rivest S. (2001). Toll-like receptor 4: The missing link of the cerebral innate immune response triggered by circulating gram-negative bacterial cell wall components. FASEB J. 15: 155–63.

Laste G, Vidor L, de Macedo IC, et al. (2013). Melatonin treatment entrains the rest-activity circadian rhythm in rats with chronic inflammation. Chronobiol Int. 30:1077–88.

Leone MJ, Chiesa JJ, Marpegan L, Golombek DA. (2007). A time to kill, and a time to heal. Pathophysiological interactions between the circadian and the immune systems. Physiol Mini Rev. 2: 60–9.

Leone MJ, Marpegan L, Bekinschtein TA, et al. (2006). Suprachiasmatic astrocytes as an interface for immune-circadian signalling. J Neurosci Res. 84:1521–7.

Leone MJ, Marpegan L, Duhart JM, Golombek DA. (2012). Role of proinflammatory cytokines on lipopolysaccharide-induced phase shifts in locomotor activity circadian rhythm. Chronobiol Int. 29:715–23.

Lin GJ, Huang SH, Chen SJ, et al. (2013). Modulation by melatonin of the pathogenesis of inflammatory autoimmune diseases. Int J Mol Sci. 14:11742–66.

Linthorst AC, Reul JM. (1998). Brain neurotransmission during peripheral inflammation. Ann N Y Acad Sci. 840:139–52.

Liu J, Malkani G, Shi X, et al. (2006). The circadian clock Period 2 gene regulates gamma interferon production of NK cells in host response to lipopolysaccharide-induced endotoxic shock. Infect Immun. 74:4750–6.

Lundkvist GB, Sellix MT, Nygard M, et al. (2010). Clock gene expression during chronic inflammation induced by infection with *Trypanosoma brucei brucei* in rats. J Biol Rhythms. 25: 92–102.

Maier SF, Goehler LE, Fleshner M, Watkins LR. (1998). The role of the vagus nerve in cytokine-to-brain communication. Ann N Y Acad Sci 840:289–300.

Marpegan L, Bekinschtein TA, Costas MA, Golombek DA. (2005). Circadian responses to endotoxin treatment in mice. J Neuroimmunol. 160:102–9.

Marpegan L, Bekinschtein TA, Freudenthal R, et al. (2004). Participation of transcription factors from the Rel/NF-kappa B family in the circadian system in hamsters. Neurosci Lett 358: 9–12.

Marpegan L, Leone MJ, Katz ME, et al. (2009). Diurnal variation in endotoxin-induced mortality in mice: Correlation with proinflammatory factors. Chronobiol Int. 26:1430–42.

Matsunaga W, Miyata S, Takamata A, et al. (2000). LPS-induced Fos expression in oxytocin and vasopressin neurons of the rat hypothalamus. Brain Res. 858:9–18.

Meza E, Juarez C, Morgado E, et al. (2008). Brief daily suckling shifts locomotor behavior and induces PER1 protein in paraventricular and supraoptic nuclei, but not in the suprachiasmatic nucleus, of rabbit does. Eur J Neurosci. 28: 1394–403.

Mogensen TH. (2013). STAT3 and the Hyper-IgE syndrome: Clinical presentation, genetic origin, pathogenesis, novel findings and remaining uncertainties. JAKSTAT. 2:e23435.

Morrow JD, Opp MR. (2005). Diurnal variation of lipopolysaccharide-induced alterations in sleep and body temperature of interleukin-6-deficient mice. Brain Behav Immun. 19:40–51.

O'Callaghan EK, Anderson ST, Moynagh PN, Coogan AN. (2012). Long-lasting effects of sepsis on circadian rhythms in the mouse. PLoS One. 7:e47087.

Okada K, Yano M, Doki Y, et al. (2008). Injection of LPS causes transient suppression of biological clock genes in rats. J Surg Res. 145:5–12.

Opp MR, Obal Jr F, Krueger JM. (1991). Interleukin 1 alters rat sleep: temporal and dose-related effects. Am J Physiol. 260: R52–8.

Opp MR, Toth LA. (1998). Somnogenic and pyrogenic effects of interleukin-1beta and lipopolysaccharide in intact and vagotomized rats. Life Sci 62:923–36.

Paladino N, Leone MJ, Plano SA, Golombek DA. (2010). Paying the circadian toll: the circadian response to LPS injection is dependent on the Toll-like receptor 4. J Neuroimmunol 225: 62–7.

Petrzilka S, Taraborrelli C, Cavadini G, et al. (2009). Clock gene modulation by TNF-alpha depends on calcium and p38 MAP kinase signaling. J Biol Rhythms. 24:283–94.

Pfeffer K, Matsuyama T, Kundig TM, et al. (1993). Mice deficient for the 55 kd tumor necrosis factor receptor are resistant to endotoxic shock, yet succumb to *L. monocytogenes* infection. Cell. 73:457–67.

Poon VY, Choi S, Park M. (2013). Growth factors in synaptic function. Front Synaptic Neurosci. 5:6.

Portaluppi F, Smolensky MH, Touitou Y. (2010). Ethics and methods for biological rhythm research on animals and human beings. Chronobiol Int. 27:1911–29.

Romanovsky AA, Sugimoto N, Simons CT, Hunter WS. (2003). The organum vasculosum laminae terminalis in immune-to-brain febrigenic signaling: a reappraisal of lesion experiments. Am J Physiol: Regul Integr Comp Physiol. 285:R420–8.

Sadki A, Bentivoglio M, Kristensson K, Nygard M. (2007). Suppressors, receptors and effects of cytokines on the aging mouse biological clock. Neurobiol Aging. 28:296–305.

Sarlis NJ, Chowdrey HS, Stephanou A, Lightman SL. (1992). Chronic activation of the hypothalamo-pituitary-adrenal axis and loss of circadian rhythm during adjuvant-induced arthritis in the rat. Endocrinology. 130:1775–9.

Scheiermann C, Kunisaki Y, Frenette PS. (2013). Circadian control of the immune system. Nat Rev Immunol. 13:190–8.

Schwartz WJ, Zimmerman P. (1990). Circadian timekeeping in BALB/c and C57BL/6 inbred mouse strains. J Neurosci. 10: 3685–94.

Seke Etet PF, Palomba M, Colavito V, et al. (2012). Sleep and rhythm changes at the time of *Trypanosoma brucei* invasion of the brain parenchyma in the rat. Chronobiol Int 29:469–81.

Shimomura K, Low-Zeddies SS, King DP, et al. (2001). Genome-wide epistatic interaction analysis reveals complex genetic determinants of circadian behavior in mice. Genome Res 11: 959–80.

Silver AC, Arjona A, Hughes ME, et al. (2012a). Circadian expression of clock genes in mouse macrophages, dendritic cells, and B cells. Brain Behav Immun. 26:407–13.

Silver AC, Arjona A, Walker WE, Fikrig E. (2012b). The circadian clock controls toll-like receptor 9-mediated innate and adaptive immunity. Immunity 36:251–61.

Simons CT, Kulchitsky VA, Sugimoto N, et al. (1998). Signaling the brain in systemic inflammation: Which vagal branch is involved in fever genesis? Am J Physiol. 275:R63–8.

Singh AK, Jiang Y. (2004). How does peripheral lipopolysaccharide induce gene expression in the brain of rats? Toxicology. 201: 197–207.

Singru PS, Sanchez E, Acharya R, et al. (2008). Mitogen-activated protein kinase contributes to lipopolysaccharide-induced activation of corticotropin-releasing hormone synthesizing neurons in the hypothalamic paraventricular nucleus. Endocrinology. 149:2283–92.

Skelly DT, Hennessy E, Dansereau MA, Cunningham C. (2013). A systematic analysis of the peripheral and CNS effects of systemic LPS, IL-1Beta, TNF-alpha and IL-6 challenges in C57BL/6 mice. PLoS One. 8:e69123.

Takahashi S, Yokota S, Hara R, et al. (2001). Physical and inflammatory stressors elevate circadian clock gene mPer1 mRNA levels in the paraventricular nucleus of the mouse. Endocrinology. 142:4910–17.

Teeling JL, Felton LM, Deacon RM, et al. (2007). Sub-pyrogenic systemic inflammation impacts on brain and behavior, independent of cytokines. Brain Behav Immun. 21:836–50.

Thompson WL, Karpus WJ, Van Eldik LJ. (2008). MCP-1-deficient mice show reduced neuroinflammatory responses and increased peripheral inflammatory responses to peripheral endotoxin insult. J Neuroinflammation. 5:35.

Waldner MJ, Foersch S, Neurath MF. (2012). Interleukin-6 – A key regulator of colorectal cancer development. Int J Biol Sci. 8: 1248–53.

Westfall S, Aguilar-Valles A, Mongrain V, et al. (2013). Time-dependent effects of localized inflammation on peripheral clock gene expression in rats. PLoS One. 8:e59808.

Yao Y, Tsirka SE. (2014). Monocyte chemoattractant protein-1 and the blood-brain barrier. Cell Mol Life Sci. 71:683–97.